Validation of the suitability of electrical impedance spectroscopy for the in-situ monitoring of nitrate in sandy soil

Xiaohu Ma, M. Sc., Luca Bifano, M. Sc., Markus Oehme, B. Sc., Prof. Dr.-Ing. Gerhard Fischerauer, University of Bayreuth, Chair of Measurement and Control Systems, Bayreuth, Germany

Abstract

This study presents the design and development of an impedance sensor to detect the nitrate concentration in soils based on the sensitivity of the soil dielectric constant to ion conductivity and on electrical double layer effects at electrodes. The impedance of samples with nitrate-nitrogen concentrations ranging from 0 to 15 mg/L was measured at frequencies between 20 Hz and 5 kHz and noticeable conductance and susceptance effects were observed. Based on the electrical impedance spectra and the known water content, two regression models using long short-term memory (LSTM) recurrent neural networks were implemented to predict the nitrate-nitrogen concentration in artificial soil (quartz sand). A coefficient of determination of $R^2 = 0.9580$ was achieved with a model including the density of the soil as a feature, and $R^2 = 0.9295$ was achieved with a model that did not include the soil density as a feature. This shows that the nitrate-nitrogen concentration could be determined almost independently of soil density. Hence, the sensing system has the potential to be used in real time and in situ to monitor nitrate concentration of soils.

Keywords: Nitrate concentration, electrochemical impedance spectroscopy, EIS, artificial neural network, ANN, LSTM

1 Introduction

Nitrate nitrogen (nitrate-N) is one of the most important nutrients for securing the yield and quality of harvested products. However, excessive content of nitrate in soil leads to environmental problems. In Germany, nitrate is the main source of pollution for the groundwater. Nationwide more than a quarter of all near-surface groundwater fails to meet the nitrate target of the European Water Framework Directive [1]. Currently, nitrate concentrations in soils are measured using the flow injection analysis [2] and spectrophotometric methods [3] in the laboratory. Both methods require expensive equipment, and the measuring processes are complicated.

Impedance spectroscopy and effective media models were used in [4]. The results demonstrate the potential of the approach, but model-based method rely on soil properties and conditions, and the individual influences of water, nitrate, and soil composition remain unclear. For this reason, the resulting error is less than satisfactory. To date, a reliable low-cost and in-situ nitrate monitoring system is still not available and much needed. This work investigates the merits of solutions based on impedance sensors.

2 Dielectric properties of soil

To be able to interpret the impact of ion concentration on the dielectric spectrum of soils, it is important to understand the dielectric properties of soils. Soil is a three-phase system, composed of the solid, liquid, and gaseous phases. This results in a dielectric constant, or relative permittivity, of between 2 and 14, depending on the soil. The liquid phase is an ion solution containing the nutrients like nitrate necessary for soil fertility and has a high static dielectric constant of between 40 and 81 at room temperature, which is strongly influenced by the ion concentration—the higher the ion concentration, the smaller the dielectric constant [5, 6]. Water is a polar liquid with distinctive dielectric relaxation and therefore has a high static dielectric constant of 81 at room temperature. With the increase of ion concentration, the ions orient the water molecules around them, thereby reducing the dielectric constant by a local high-field effect [6].

In an electric A-C field, energy is absorbed and stored in soil-solution mixtures. The effect of energy storage is connected with the real part $\varepsilon'(\omega)$ of the permittivity, while the energy absorption is connected with the imaginary part $\varepsilon''(\omega)$ of the permittivity. Here, ω denotes the angular frequency.

Figure 1 shows a schematic representation of dielectric losses in soils as a function of frequency [7]. Various effects contribute to the complex dielectric constant. It is obvious that the ionic conductivity and the double-layer effect play major roles in the imaginary part of the soil permittivity at lower frequencies. Both effects are positively correlated to the ion concentration [8]. At the same time the double-layer effect leads to a frequency-dependent capacitance, which also influences the real part of the permittivity [8].

ISBN 978-3-8007-5835-7

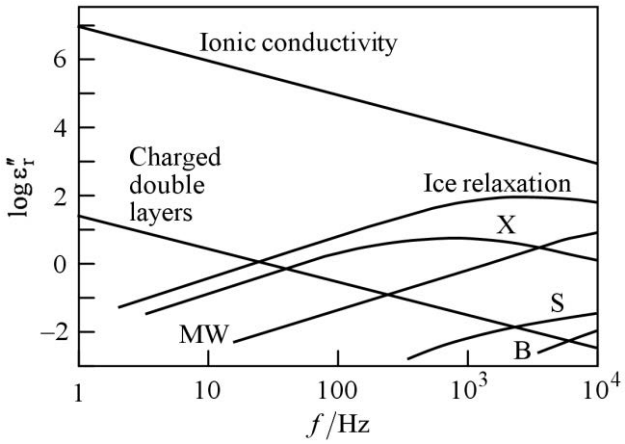

Fig. 1 Contributions to the imaginary part $\varepsilon_r'' = \varepsilon''/\varepsilon_0$ of the relative permittivity of soil (after [7]). B: Bound water relaxation; MW: Maxwell-Wagner effect; S: Surface conductivity; X: Crystal water relaxation.

3 Measuring the impedance of soil samples

As material under test (MUT), dry quartz sand with six different nitrate-N concentrations was examined, viz., 0, 2, 4, 6, 8, and 10 mg/kg. 500 g of pure quartz sand were enriched in a beaker with sodium nitrate solutions prepared according to international standards [2]. After mixing and drying, the sand-nitrate mixture was examined at different water contents (the deionized water concentrations were between 0 and 150 g/kg). The water content here is the ratio of the mass of water and mass of dry mixture. Dry-mixture mass is expressed by the mass of mixture dried (up to the constant weight) at 105 °C. In agriculture, the mass water content is not used frequently but a necessary step for the measurement of volumetric water content with gravimetric methods, as will be seen later. In the field, the volumetric water and nitrate-N contents offer more information about the ratio of pores filled with water and make it easier to calculate the quantity of water and nitrate in an area. So the above mentioned water and nitrate-N mass contents were converted to volumetric contents by

$$\theta_W = \frac{m_W}{V} = \frac{m_S \cdot \omega_W}{V} = \rho_S \cdot \omega_W \quad \text{and} \qquad (1)$$

$$\theta_N = \frac{m_N}{V} = \frac{m_S \cdot \omega_N}{V} = \rho_S \cdot \omega_N \,. \qquad (2)$$

where θ_W and θ_N respectively are the volumetric water and nitrate-N contents, ω_W and ω_N are the corresponding mass contents, m_W, m_N and m_S are the masses of water, nitrat-N, and sand in the measurement volume V, and ρ_S is the density of dry sand in the measuring cell. Obviously, even when the mass content remains constant, the volumetric content can vary.

To investigate various soil mixtures, the measuring cell shown in Figure 2 was used. It consists of two opposing square plates made of PTFE with a side length of 15 cm and two circular stainless steel electrodes with a diameter of 13 cm centered in them, forming a plate capacitor with an electrode spacing of 1 cm. The MUTs were filled into the space between the electrodes until the material was flush with the top edge of the measuring cell. Care was taken to keep the bulk density as planned.

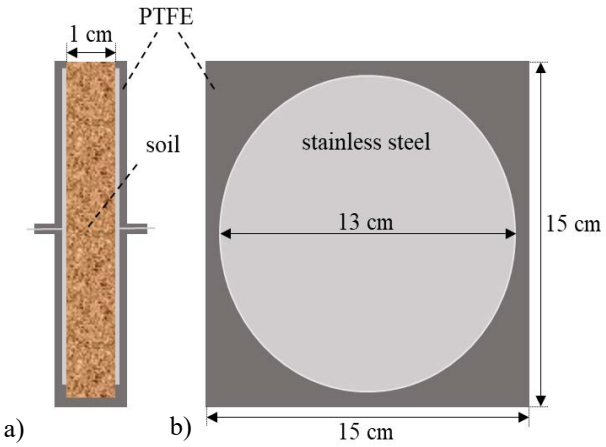

Fig. 2 Parallel-plate impedance sensor. a) Cross section. b) View of the right plate from the left.

The impedance $\underline{Z} = |\underline{Z}|e^{j\varphi} = R + jX$ was measured over a frequency range from 20 Hz to 5 kHz using an Agilent E4980A LCR meter (98 measurement points per frequency sweep). For electrochemical systems, lower frequencies (as low as 1 mHz) would provide more information, but would also take more time for the measurement. Therefore, as we are interested in fast measurements over larger areas (agricultural fields), we restricted the frequency to values above 20 Hz. At each frequency, both the apparent impedance $|\underline{Z}|$ and the impedance phase φ were recorded and then evaluated in Matlab. Each MUT was repeatedly measured 20 times.

Figure 3 shows the measured frequency-dependent conductance $G = \mathrm{Re}\{\underline{Y}\} = \mathrm{Re}\{1/\underline{Z}\}$ as a function of nitrate-N and water concentrations. G increases with increasing nitrate-N and water contents, with the nitrate-N sensitivity being significantly greater than the moisture sensitivity. This demonstrates the potential for in-situ monitoring of the nitrate-N concentration in soil with water as influence quantity, but also emphasizes the need for prior calibration.

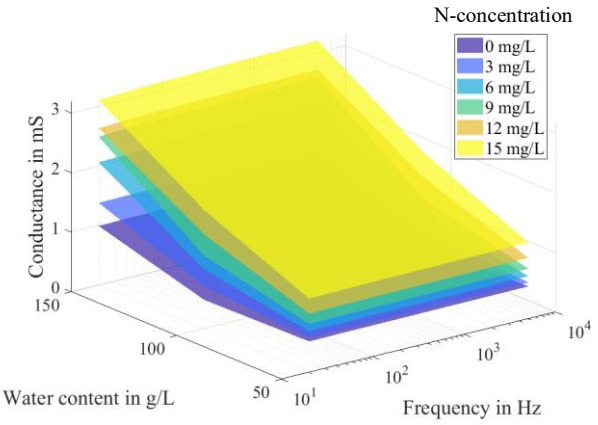

Fig. 3 Measured test cell conductance as a function of the nitrate-N concentration (in mg/L) and of the water content (in g/L) in artificial soil (quartz sand), and of frequency.

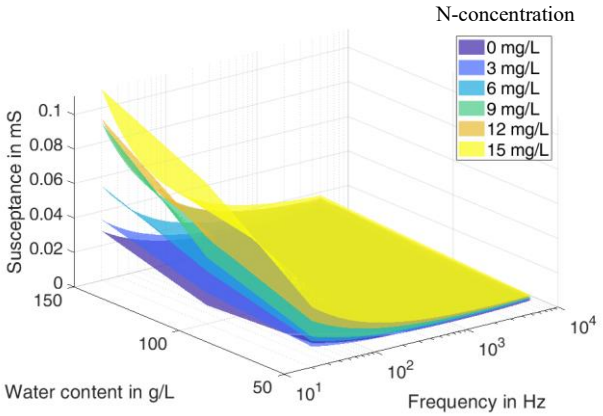

Fig. 4 Measured test cell susceptance as a function of the nitrate-N concentration (in mg/L) and of the water content (in g/L) in artificial soil (quartz sand), and of frequency.

Likewise, Figure 4 shows the measured frequency-dependent susceptance $B = \mathrm{Im}\{\underline{Y}\} = \mathrm{Im}\{1/\underline{Z}\}$ as a function of nitrate-N and water concentrations. In the low-frequency region from 20 Hz to 1 kHz, B increases with increasing nitrate-N and water contents. This can be explained by the electrical double-layer effect, which is strongly related to the ion concentration [8]. It may provide a possibility to monitor the nitrate-N concentration at low frequencies.

4 Evaluation with LSTM

The data in Figs. 3 and 4 suggest that the designed impedance sensor can measure the nitrate-N concentration, possibly with prior calibration. It may have the potential to monitor the nitrate-N concentration in soils in situ. As calibrations to take into account specific soil types and water content are likely to require too much time and effort, we looked for ways to get rid of the need for calibration. The reasoning is about the following: impedance spectra contain an abundance of signal features. This richness of information should allow one to estimate both analyte concentrations and influence quantity values (soil density, water content, etc.). The estimation must be automated, which calls for a machine-learning algorithm.

We followed this line of reasoning and used long short-term memory (LSTM) recurrent neural networks (ANN) to build regression models to detect the nitrate-N in sandy soils. The LSTM networks are capable of learning long term dependencies [9], which makes them attractive for the evaluation of impedance spectra.

Before the model training, the input data were centered and scaled to have zero mean and standard deviation 1. Then the impedance at each frequency was passed to a memory cell (Fig. 5). In Fig. 5, σ and tanh respectively denote the activation functions $(1 + \mathrm{e}^{-x})^{-1}$ and $\tanh(x)$, and $f_f, i_f, o_f, \tilde{c}_f$ respectively represent the forget gate, input gate, output gate, and cell candidate at the frequency f. C_f and h_f are the cell state and hidden state. U_f is the input data of the frequency sequence. The hidden state is passed to the next ANN layer as input.

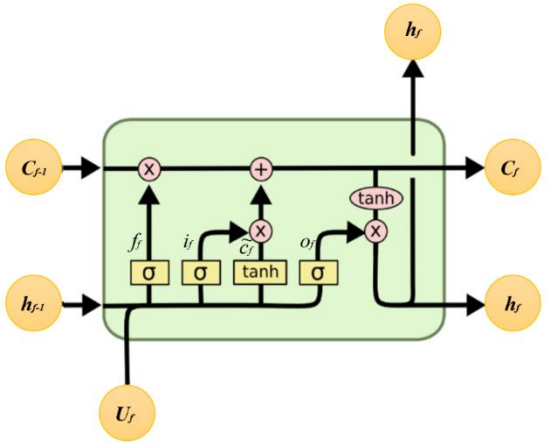

Fig. 5 LSTM memory cell.

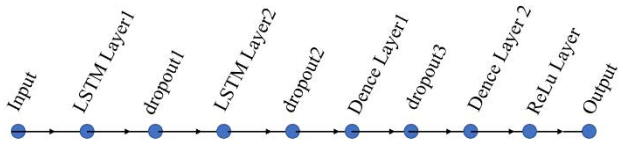

Fig. 6 LSTM networks structure.

Various LSTM recurrent ANN architectures were tested with different numbers of LSTM layers, hidden units, and dense layers. The final architecture comprised two LSTM layers and two dense layers with drop-out between the layers. An additional layer in front of the output layer (denoted as ReLu Layer in Fig. 6) is used to secure a positive output. Our impedance measurements provided 2520 spectra (126 sand compositions × 20 repetitions). These were split into training and validation data in the ratio 80:20. After the training process, the ANN model was tested using 360 spectra unused up to this point. Hyperparameters including batch size, units of each ANN layer, and solvers were tuned until satisfactory results were found.

Two regression models using the above-mentioned structure were tested. The first one takes the impedance data, soil density ρ_b, and volumetric water content θ_W as features. To be more specific, the feature vector was

$$U_f = (B_f, G_f, \rho_b, \theta_W, X_f, R_f, |\underline{Z}|_f, \varphi_f). \quad (3)$$

The other model did not include density as a feature. Hence, the feature vector in this case was

$$U_f' = (B_f, G_f, \theta_W, X_f, R_f, |\underline{Z}|_f, \varphi_f). \quad (4)$$

Both models were tested using identical parameters. For brevity's sake, we only present results for the following parameter values: respective number of neurons in the two hidden layers (LSTM layers): 77 and 45; batch size: 16; respective number of neurons in the two dense layers: 25 and 1.

The performance of the two models is illustrated in Fig. 7. To quantify the results, the coefficient of determination R^2 between actual nitrate-N concentration and concentration estimated from the measured impedance spectra was computed by

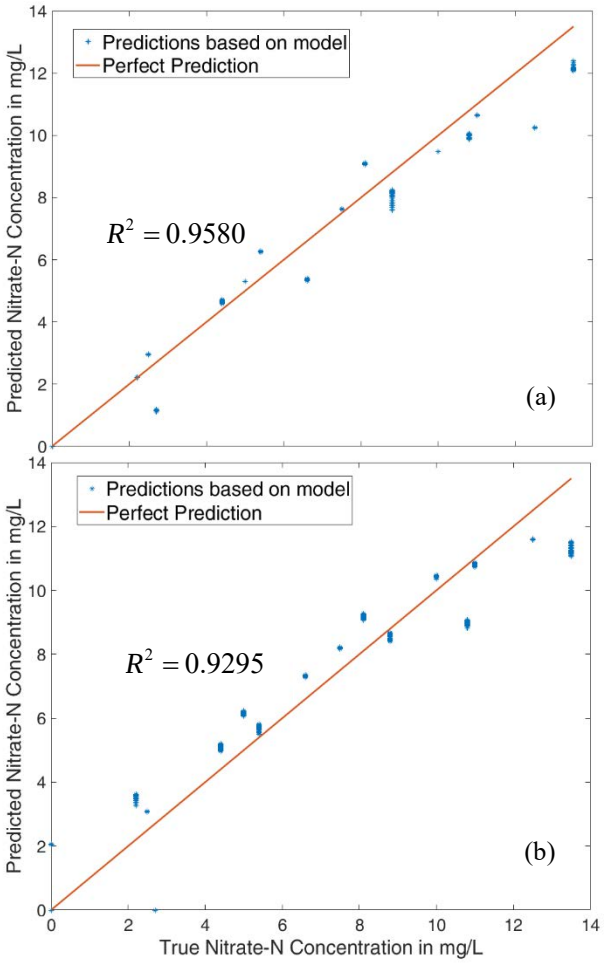

Fig. 7 Nitrate-N concentrations predicted from impedance spectra by LSTM-ANN with soil density (a) included and (b) excluded as feature (model 1 and 2, respectively).

$$R^2 = 1 - \frac{\sum_i (V_{test-i} - V_{pre-i})^2}{\sum_i (V_{test-i} - \overline{V_{test}})^2}. \qquad (5)$$

Here, i is the case index, V_{test-i} and V_{pre-i} are the actual and predicted nitrate-N concentrations of the test data, respectively, and $\overline{V_{test}}$ is the mean of the actual concentration. Both models predict the concentration very well with $R^2 = 0.9580$ for model 1 and $R^2 = 0.9295$ for model 2. The maximum allowed nitrate-N concentration in arable soil is about 50 and 150 mg/L at depths of 30 and 90 cm, respectively. A measurement based on the approach investigated can clearly resolve such values very well. And, although model 1 performs slightly better, the described LSTM neural networks are able to learn the relationship between impedance spectra, water content, and nitrate-N concentration even when the soil density is unknown.

5 Conclusion

Our results demonstrate that nitrate-N concentrations of soils can be estimated from measured impedance spectra of soil samples with errors that are compatible with field requirements (well below the maximum allowed concentrations). They also demonstrate that this estimation is robust against important influence quantities such as soil density when the impedance data are evaluated with LSTM recurrent artificial neural networks.

Our further goal is to conduct more experiments to expand the measuring range and include more soil types like potting soils, brown soils, and clay mixtures. In this way, we hope to implement a method based on machine learning that is capable of measuring nitrate-N concentrations virtually independent of soil properties. We are aware, however, that true field measurements cannot rely on bulky and expensive laboratory equipment, but require application-specific printed-circuit-board impedance spectrometers.

Acknowledgment

The authors gratefully acknowledge funding by the Volkswagen Foundation. The data used in this paper is available under the DOI: 10.15495/do_ubt_2067.

Literature

[1] Jakobs, I.; et al.: Nitratbericht 2020: Gemeinsamer Bericht der Bundesministerien für Umwelt, Naturschutz und nukleare Sicherheit sowie für Ernährung und Landwirtschaft [= Nitrate Report 2020: Joint Report of the Federal Ministries for …; in German]. Bonn, Germany: German Ministry for Food and Agriculture and German Ministry for the Environment, Nature Conservation and Nuclear Safety, May 2020.

[2] EN ISO 13395:1996-07: Water quality – Determination of nitrite nitrogen and nitrate nitrogen and the sum of both by flow analysis (CFA and FIA) and spectrometric detection. Brussels, Belgium: CEN, 1996.

[3] Narayana, B.; Sunil, K.: A spectrophotometric method for the determination of nitrite and nitrate. Eurasian J. Anal. Chem. 4 (2), Aug. 2009, pp. 204–215.

[4] Pandey, G.; Kumar, R.; Weber, R. J.: Real time detection of soil moisture and nitrates using on-board in situ impedance spectroscopy. Proc. IEEE Int'l Conf. Systems, Man, and Cybernetics (SMC), Manchester, England, Oct. 13–16, 2013, pp. 1081–1086.

[5] Kanoun, O.; Tetyuev, A.; Tränkler, H.: Bodenfeuchtemessung mittels Impedanzspektroskopie [= Soil moisture measurement with impedance spectroscopy; in German]. TM 71 (9), Sept. 2004, pp. 475–485.

[6] Nir, G.; Keith, P.: Dependence of the dielectric constant of electrolyte solutions on ionic concentration: A microfield approach. Phys. Rev. E 94, 2016, art. no. 012611.

[7] Hasted, J. B.: Aqueous Dielectrics. London: Chapman and Hall, 1973, pp. 238–252.

[8] Ben Ishai, P; et al.: Electrode polarization in dielectric measurements: a review. Meas. Sci. Technol. 24 (10), Oct. 2013, art. no. 102001.

[9] Hochreiter, S.; Schmidhuber, J.: LSTM can solve hard long time lag problems. Proc. 10th Annual Conf. Neural Inform. Proc. Syst. (NIPS), Denver, CO, Dec. 2–5, 1996, pp. 473–479.